Settling the Half-Life of ^{60}Fe: Fundamental for a Versatile Astrophysical Chronometer

A. Wallner,[1,2] M. Bichler,[3] K. Buczak,[2,3] R. Dressler,[4] L. K. Fifield,[1] D. Schumann,[4] J. H. Sterba,[3]
S. G. Tims,[1] G. Wallner,[5] and W. Kutschera[2]

[1]*Department of Nuclear Physics, Australian National University, Canberra, Australian Capital Territory 2601, Australia*
[2]*VERA Laboratory, Faculty of Physics, University of Vienna, 1090 Vienna, Austria*
[3]*Atominstitut, Vienna University of Technology, 1020 Vienna, Austria*
[4]*Biology and Chemistry, Paul Scherrer Institute (PSI), 5232 Villigen, Switzerland*
[5]*Institute of Inorganic Chemistry, University of Vienna, 1090 Vienna, Austria*

In order to resolve a recent discrepancy in the half-life of ^{60}Fe, we performed an independent measurement with a new method that determines the ^{60}Fe content of a material relative to ^{55}Fe ($t_{1/2} = 2.744$ yr) with accelerator mass spectrometry. Our result of $(2.50 \pm 0.12) \times 10^6$ yr clearly favors the recently reported value $(2.62 \pm 0.04) \times 10^6$ yr, and rules out the older result of $(1.49 \pm 0.27) \times 10^6$ yr. The present weighted mean half-life value of $(2.60 \pm 0.05) \times 10^6$ yr substantially improves the reliability as an important chronometer for astrophysical applications in the million-year time range. This includes its use as a sensitive probe for studying recent chemical evolution of our Galaxy, the formation of the early Solar System, nucleosynthesis processes in massive stars, and as an indicator of a recent nearby supernova.

The neutron-rich radionuclide ^{60}Fe is of growing importance for our understanding of stellar and interstellar processes in the million-year time range, largely boosted by the recent observation of galactic γ-rays from its radioactive decay and the discovery of live ^{60}Fe on Earth, probably originating from a nearby supernova (SN). There is a range of astrophysical applications which require an accurate value of the ^{60}Fe half-life for proper tracing of its nucleosynthetic history and production: (i) ^{60}Fe is a neutron-rich iron isotope just beyond the end of thermonuclear stellar burning, where neutron capture begins to dominate heavy-element nucleosynthesis [1]. Its production is thus sensitive to the neutron environment under different stellar conditions. (ii) Diffuse ^{60}Fe emissions in the Galaxy were observed through the 1173-and 1332-keV γ-lines from the decay of its daughter ^{60}Co by the space-born International-Gamma-Ray-Astrophysics-Laboratory (INTEGRAL) [2,3], providing evidence for recent and ongoing nucleosynthesis in the Galaxy. (iii) The presence of ^{60}Fe in the early Solar System (ESS) can be traced through the measurement of ^{60}Ni isotopic anomalies in meteorites [4–12], complementing information obtained from other extinct radionuclides [13]. Furthermore, ^{60}Fe, like ^{26}Al, was suggested as a major heat source for the first compact objects in the ESS [4,14]. (iv) The discovery of live ^{60}Fe in a deep-sea manganese crust [15,16] opened the possibility of gauging late and close-lying SN events, and prospects for finding this signal in sediments [17–19] and in biogenic material [19] were discussed.

^{60}Fe is separated from the closest stable Fe-isotope, ^{58}Fe, by the short-lived ^{59}Fe ($t_{1/2} = 44.5$ days). The double neutron capture process, its dominant production path, has to bridge ^{59}Fe before it decays. Thus, its stellar production requires sufficient neutron densities. Massive star interiors and supernovae (SNe) are candidate sources where it is predominately produced in the late shell-burning phase before the core collapse [3]. Presumably within SN explosions, possibly with super-AGB stars contributing at lower rates [20], ^{60}Fe is ejected into the interstellar medium (ISM). The nucleosynthetic yields are still uncertain although laboratory experiments recently became feasible for studying production and destruction of ^{60}Fe [1].

For properly interpreting the above-mentioned astrophysical scenarios, an accurate and precise ^{60}Fe half-life value is needed. Furthermore, the beta-minus decay of ^{60}Fe provides a clock independent of its ionization state in a stellar environment, in contrast to electron-capture decays (^{7}Be, ^{44}Ti, ^{53}Mn, ^{56}Ni, ^{57}Co) [21].

Early interest in an accurate half-life value for ^{60}Fe came from studies of extinct radioactivities in the ESS [22]. At that time, a value of $\sim 3 \times 10^5$ yr was available, uncertain by a factor of 3 [23]. Later, a potentially considerably longer half-life was discussed [24].

The decay scheme in Fig. 1 [25,26] shows that ^{60}Fe decays via the short-lived ^{60m}Co-isomer ($t_{1/2} = 10.467$ min) almost 100% to the ^{60g}Co ground-state ($t_{1/2} = 5.2712 \pm 0.0004$ yr). Therefore, a direct determination of the ^{60}Fe half-life can be performed by measuring the ingrowth of the ^{60g}Co activity for a few years from a material with a known number of ^{60}Fe atoms, initially purified from ^{60g}Co. This ingrowth can be measured through the 1173-keV($4_1^+ \rightarrow 2_1^+$) and/or the 1332-keV($2_1^+ \rightarrow 0^+$) γ-ray transitions in ^{60}Ni. Since there are two small feeding branches from ^{60m}Co to the first and second 2^+ states in ^{60}Ni, the intensity of the 1332-keV γ-ray is slightly enhanced relative to the
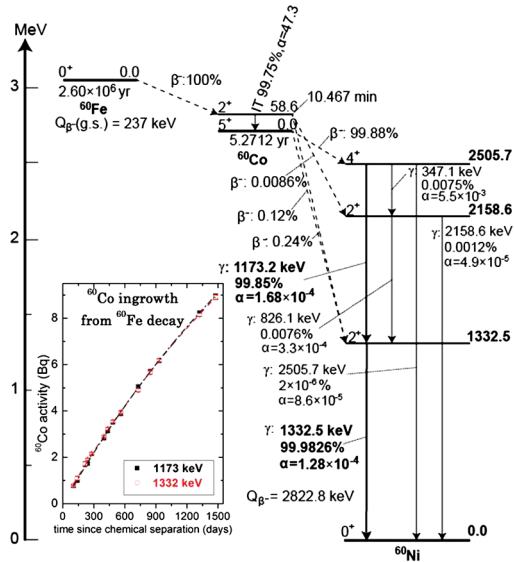
FIG. 1 (color online).   The decay scheme of ^{60}Fe through ^{60}Co to ^{60}Ni, and the ^{60}Co ingrowth measurement (inset). All data are from Refs. [25,26], except for the half-life of ^{60}Fe, which is the mean value of Ref. [28] and of the current work. Inset: ingrowth of the ^{60g}Co activity from the decay of ^{60}Fe observed through the 1173.2 keV (squares) and the 1332.5 keV (circle) γ-transitions in ^{60}Ni. Measurements were performed for a period of 4 yr after separation of ^{60g}Co from ^{60}Fe. The lines are fits to the data points by Eqs. (1a) and (1b), respectively.

^{60g}Co decay. The connection between the ingrowth of these two γ-ray intensities to the ^{60}Fe activity is described to good approximation (the ^{60}Fe activity does not change during the measurement) by

$$A_{1173}(t) = 0.9985[A_0 e^{-\lambda t} + 0.9975 A_{60Fe}(1 - e^{-\lambda t})], \quad (1a)$$

$$A_{1332}(t) = 0.9998[A_0 e^{-\lambda t} + A_{60Fe}(1 - 0.9975 e^{-\lambda t})], \quad (1b)$$

where $A(t)$ is the γ-ray yield of ^{60}Co measured through the 1173-keV and 1332-keV γ-rays, respectively (Fig. 1). A_0 is the activity of ^{60g}Co at $t = 0$, λ the decay constant of ^{60g}Co, and A_{60Fe} the ^{60}Fe activity. If the number of ^{60}Fe-atoms N_{60Fe} is known, the half-life of ^{60}Fe can be calculated from

$$t_{1/2}(^{60}\text{Fe}) = \ln 2 \times N_{60Fe}/A_{60Fe}. \quad (2)$$

The first ^{60}Fe half-life measurement utilizing this method was in 1984 [27]. ^{60}Fe was produced from a 19-mAh bombardment of a copper disk with 191-MeV protons at the Brookhaven Linac Isotope Producer (BLIP). After a cool-down period of 1 yr, iron was separated and ^{60}Fe/^{nat}Fe atom ratios of 9.5×10^{-8} were measured with accelerator mass spectrometry (AMS) at the Argonne Tandem Linear Accelerator System (ATLAS). The sample for the ^{60}Co activity measurement contained 4.0×10^{14} ^{60}Fe atoms. These measurements resulted in the half-life value of $(1.49 \pm 0.27) \times 10^6$ yr [27] (Table I).

For the second measurement [28], 10 times more ^{60}Fe was available (5.9×10^{15} atoms), extracted from a proton-irradiated copper beam dump (590 MeV, $\sim$100 mAh, 12 yr cooling) at the Paul-Scherrer-Institute (PSI) [30]. Details of iron extraction and the measurement of ^{60}Fe/^{nat}Fe atom ratios of $\sim 2 \times 10^{-4}$ with multicollector-inductively coupled plasma mass spectrometry (MC-ICPMS) are described in recent papers [29,30]. Combined with the ^{60g}Co ingrowth measurement, a significantly longer half-life of $(2.62 \pm 0.04) \times 10^6$ yr was obtained [28]. Clearly, the disagreement of these two values called for independent new measurements with the goal to clarify the existing discrepancy. Thus, new ^{60}Fe sample material was prepared at PSI. Part of this material was used for the measurement described in the present Letter. We note two additional half-life measurements are ongoing with the remainder of the new ^{60}Fe material, at PSI [31] and the University of Notre Dame [32].

Both previous measurements combined a ^{60g}Co ingrowth measurement with an absolute ^{60}Fe/^{nat}Fe isotope-ratio measurement. Applying AMS [33,34] completely removes any molecular isobaric interference, and in addition allows the separation of the omnipresent atomic isobar ^{60}Ni using well-established particle detection techniques. AMS measures isotope ratios, here radionuclide (^{60}Fe) versus stable isotope (^{56}Fe). AMS ratios are normalized via standards to correct for differing beam losses and deficiencies in the current measurements (^{56}Fe). However, the nominal values of standards are commonly related to the half-life, a fact that excludes their use in half-life measurements.

TABLE I.   Quantities in two previous [27,28] and the current experiments used to calculate the half-life from Eq. (2).

Reference	Origin of sample	^{60}Fe determination	^{60}Fe/^{nat}Fe measured	N_{60Fe}	A_{60Fe}	$t_{1/2}$ (^{60}Fe)
[27]	Cu disk BLIP	AMS at ANL: ^{60}Fe/^{nat}Fe absolute	$(9.54 \pm 1.40) \times 10^{-8}$	$(3.99 \pm 0.71) \times 10^{14}$	(8.8 ± 1.6) Bq	$(1.49 \pm 0.27) \times 10^6$ yr
[28]	Cu beam dump PSI	ICPMS at PSI: ^{60}Fe/^{nat}Fe absolute	$(2.048 \pm 0.004) \times 10^{-4}$	$(5.873 \pm 0.020) \times 10^{15}$	(49.25 ± 0.08) Bq[a]	$(2.62 \pm 0.04) \times 10^6$ yr
This work	Cu beam dump PSI	AMS at ANU: ^{60}Fe/^{55}Fe	$(1.88 \pm 0.08) \times 10^{-9}$[b]	$(2.47 \pm 0.11) \times 10^{15}$	(21.72 ± 0.35) Bq	$(2.50 \pm 0.12) \times 10^6$ yr

[a]Kivel *et al.* [29] quote (49.57 ± 0.53) Bq and $(5.873 \pm 0.050) \times 10^{15}$ atoms.
[b]This number is a secondary number and is deduced from our primary data (for details see text).

A drawback in AMS is thus a complex measurement setup with the consequence of uncertainties for absolute ^{60}Fe counting. ICPMS also largely gets rid of molecular interferences, but requires subtraction of the contribution from the stable atomic isobar ^{60}Ni, which could not be distinguished from ^{60}Fe. This ^{60}Ni contribution was determined from simultaneous measurements of the neighboring isotopes. Because the initial Ni composition of the beam-dump material used in Ref. [28] differed substantially from the natural relative abundances, it was necessary to dilute it back to the natural composition by repeated addition and chemical removal of ^{nat}Ni. The final corrections on the $A = 60$ isobar were $\sim15\%$ [28,29,35].

Here, we have followed Ref. [27] in using AMS for determining the number of ^{60}Fe atoms to exclude all molecular and atomic isobaric interferences. However, our new approach was to utilize the $^{60}Fe/^{55}Fe$ atom ratio, i.e., a ratio of two radionuclides of about the same concentration and counted with the same detector, which had the advantage that systematic uncertainties and corrections were largely reduced by using the same detection setup. We note a somewhat similar measurement of the ^{146}Sm half-life [36] using (naturally existing) ^{147}Sm ($t_{1/2} = 1.06 \times 10^{11}$ yr) as reference (however, high concentrations required quantitative beam attenuation).

The material for the current work originates from the same copper beam dump as used in Ref. [28], but from a different fraction, which was first used to measure the stellar $^{60}Fe(n,\gamma)^{61}Fe$ cross section [1], and afterwards again purified from in-grown ^{60g}Co. Data produced in the work here are based on different methods and completely independent of Ref. [28]. About one third of the $^{60}Fe(n,\gamma)$ material recovered at PSI was used in the present work. It contained $\sim3.5 \times 10^{15}$ ^{60}Fe atoms in 1.00027 g of a $0.1M$ HCl solution together with a ^{55}Fe activity of ~4–5 MBq ($\sim5 \times 10^{14}$ atoms). The stable iron content was $< 125\ \mu g$. A fraction from this master solution (0.65005 g) was used for the ^{60g}Co ingrowth activity measurement with a total accumulation time of 4 yr [A_{60Fe} in Eq. (2)]. Another fraction (0.30120 g) was used for the determination of the number of ^{60}Fe atoms, N_{60Fe}, via AMS at the Australian National University (ANU). The

concentration of the original solution was $^{60}Fe/^{nat}Fe >$ 0.8×10^{-3}. In order to avoid contamination of the ion source with ^{60}Fe, that would have compromised ongoing measurements for the search for a ^{60}Fe supernova signature in terrestrial archives [15–19] at the $^{60}Fe/Fe \sim$ 10^{-16} level, we had to dilute that material by several orders of magnitude with ^{nat}Fe. While the γ-ray measurement is a well-known procedure, the determination of the number of ^{60}Fe atoms requires special attention, and probably was the cause of the disagreement of the two previous half-life measurements [27,28].

Figure 1 shows the result of the ingrowth measurement of ^{60g}Co, which was performed at the Vienna University of Technology. The 0.65005 g fraction of the master solution was filled up to 3 ml with triply distilled H_2O and mounted in a plastic bottle at a distance of 8.2 cm above a high-purity Ge detector (50% relative efficiency, 2.0 keV resolution at 1332 keV). The efficiency was determined with a mixed-radionuclide calibration source (QCY48, $\pm1.5\%$) from Amersham, in 3 ml triply distilled H_2O to obtain the same geometry as for the ^{60}Fe sample. The efficiencies were $(3.093 \pm 0.048) \times 10^{-3}$ for 1173 keV and $(2.826 \pm 0.044) \times 10^{-3}$ for 1332 keV.

From the fit of Eq. (1a) to the ingrowth of the 1173-keV line, one obtains $A_0 = (0.02 \pm 0.03)$ Bq and $A_{60Fe} = (21.55 \pm 0.37)$ Bq, and of Eq. (1b) (1332 keV) $A_0 = (-0.03 \pm 0.03)$ Bq and $A_{60Fe} = (21.89 \pm 0.38)$ Bq, i.e., an average ^{60}Fe activity $A_{60Fe} = (21.72 \pm 0.35)$ Bq (uncertainty includes measurement and calibration source).

The dilution series for the AMS measurements is detailed in Table II. The number of ^{55}Fe and ^{60}Fe atoms was reduced by a factor of exactly 10 at each step (Fe-1 to Fe-4). Only sample Fe-4 with the lowest ^{60}Fe content was used for ^{60}Fe AMS at the ANU (see below). Rather than trying to measure the $^{60}Fe/^{56}Fe$ ratio absolutely as in Ref. [27], we took advantage of the presence of a second radionuclide in the same material and determined ^{60}Fe relative to ^{55}Fe. The half-life of ^{55}Fe is well-known ($\pm0.3\%$) [37], we recently produced an AMS standard [38], and ^{55}Fe is easily measured with AMS [39,40]. Equation (3) details our method for determining the number of ^{60}Fe atoms in Fe-1, $N_{60}(Fe\text{-}1)$,

TABLE II. Dilution series for ^{55}Fe beta activity (LSC) and $^{55}Fe/^{56}Fe$ atom-ratio measurements (AMS).

Sample name	Fe carrier[a] (mg)	N_{56} (^{56}Fe at) ($\times10^{20}$)	Dilution factor for $^{55,60}Fe$	N_{60}/N_{56} relative to Fe-1	N_{55}/N_{56} relative to Fe-1	$^{55}Fe/^{56}Fe$ (AMS measured; VERA)[b]	$^{55}Fe/^{56}Fe$ (AMS) relative to Fe-1	^{55}Fe activity[c] (Bq/g)
Fe-1	50.0	4.95	1	1	1	$(4.64 \pm 0.09) \times 10^{-7}$	1	22185 ± 755
Fe-2	55.0	5.44	10	0.091	0.091	$(4.37 \pm 0.06) \times 10^{-8}$	0.094 ± 0.002	2230 ± 79
Fe-3	55.5	5.49	100	0.0090	0.0090	$(4.30 \pm 0.14) \times 10^{-9}$	0.0093 ± 0.0004	217 ± 7
Fe-4	55.55	5.50	1000	0.00090	0.00090	$(4.35 \pm 0.18) \times 10^{-10}$	0.00094 ± 0.00004	22 ± 1

[a]Fe standard solution with 1 mg Fe/ml.
[b]Not normalized to standard.
[c]LSC measurements from 100 μl aliquots of the 100-ml samples relative to a ^{55}Fe reference material [38] valid for 01/01/2010.

$$N_{60}(\text{Fe-1}) = N_{60}(\text{Fe-4}) \times \frac{N_{60}(\text{Fe-1})}{N_{60}(\text{Fe-4})} = N_{60}(\text{Fe-4}) \times \frac{N_{55}(\text{Fe-1})}{N_{55}(\text{Fe-4})}$$

$$= \underbrace{\frac{R_{60/56}(\text{Fe-4})}{R_{55/56}(\text{Fe-4})}}_{(a)} \times \underbrace{\frac{R_{55/56}(\text{Fe-4})}{R_{55/56}(A0)}}_{(b)} \times \underbrace{R_{55/56}(A0)}_{(c)} \times \underbrace{N_{56}(\text{Fe-4})}_{(d)} \times \underbrace{\frac{N_{55}(\text{Fe-1})}{N_{55}(\text{Fe-4})}}_{(e)} \qquad (3)$$

where $R_{60/56}$, for example, means the measured AMS isotope ratio $N_{60\text{Fe}}/N_{56\text{Fe}}$. The factors (a)–(e) of Eq. (3) were determined as follows: (a) Relative quantity measured by AMS at ANU. (b) The $^{55}\text{Fe}/^{56}\text{Fe}$ ratio in Fe-4 [$R_{55/56}$ (Fe-4)] was measured relative to a ^{55}Fe standard ($A0$) by AMS at VERA and ANU, and by liquid scintillation counting (LSC). (c) $R_{55/56}$ of the ^{55}Fe standard was calculated from a certified ^{55}Fe solution of accurately known activity ($\pm 1.5\%$, No. 2000-1215 PTB-Braunschweig, Germany [38]). (d) The number of ^{56}Fe atoms in Fe-4 was derived from the known concentration of the iron standard solution used for the dilutions. (e) The relative numbers of ^{55}Fe atoms in Fe-1 and Fe-4 were derived from the dilutions, and checked by AMS at VERA and by LSC.

To summarize, absolute measurements were avoided through relative AMS measurements of N_{60}/N_{55} ($= R_{60/56}/R_{55/56}$) as well as of ^{55}Fe relative to the ^{55}Fe standard. Thus, possibly unknown systematic uncertainties are expected to cancel largely in our approach. Furthermore, from LSC we measured directly the ^{55}Fe activity of Fe-1, $A_{55}(\text{Fe-1})$ and combined it with the $^{55,60}\text{Fe}$ measurements,

$$N_{60}(\text{Fe-1}) = A_{55}(\text{Fe-1}) \times \frac{t_{1/2}(^{55}\text{Fe})}{\ln 2} \times \frac{N_{60}}{N_{55}} \qquad (4)$$

with N_{60}/N_{55} the quantity (a) in Eq. (3). All ^{60}Fe AMS measurements were performed at the ANU heavy ion accelerator facility [41–43]. A strong background from stable ^{60}Ni prevents the measurement of ^{60}Fe at smaller facilities. The gas-filled magnet technique [44] was employed for spatially separating ^{60}Ni isobars from ^{60}Fe at particle energies of ~160 MeV (Fig. 2). In this setup, both ^{55}Fe and ^{60}Fe were required to follow the same trajectory in the gas-filled-magnet by adjusting the magnetic field so that both entered the final detector at the same position, as verified by position-sensing electrodes. Hence, any loss of ^{60}Fe ions in the magnet would be identical for ^{55}Fe and will cancel in the $^{60}\text{Fe}/^{55}\text{Fe}$ isotope ratio. $R_{60/56}$ (Fe-4) was measured in three beam times using both 10^+ and 11^+ ions at the high-energy side of the spectrometer. After correcting with the measured 10^+ and 11^+ charge-state yields [41,42], they agree well and indicate a ~3% uncertainty in AMS. $R_{55/56}$ (Fe-4) was measured relative to the AMS standard in two measurement series, again analyzing the 10^+ and 11^+ charge states [41]. In both cases, $R_{55/56}(\text{Fe-4})/R_{55/56}(A0)$ was 0.93 ± 0.06 (see the Supplemental Material [41].

AMS measurements of the $R_{55/56}$ ratios of Fe-1 to Fe-4 and $A0$ [factors (b) and (e)] were performed at the 3-MV AMS facility VERA [38]. Atomic Fe^- ions from the ion source were selected because the stable isobar ^{55}Mn does not form negative ions [39,40] and hence does not interfere with ^{55}Fe counting [41,42]. This makes it possible to measure ^{55}Fe at the lower energies (≤ 24 MeV) available at VERA but with higher precision compared to the more complex ANU setup. The ^{55}Fe results for the dilution series from both LSC and AMS are shown in Table II. They demonstrate the linearity of the dilution. Furthermore, the ratio of the number of ^{55}Fe atoms in Fe-4 and the $A0$ standard was deduced from AMS at VERA to be
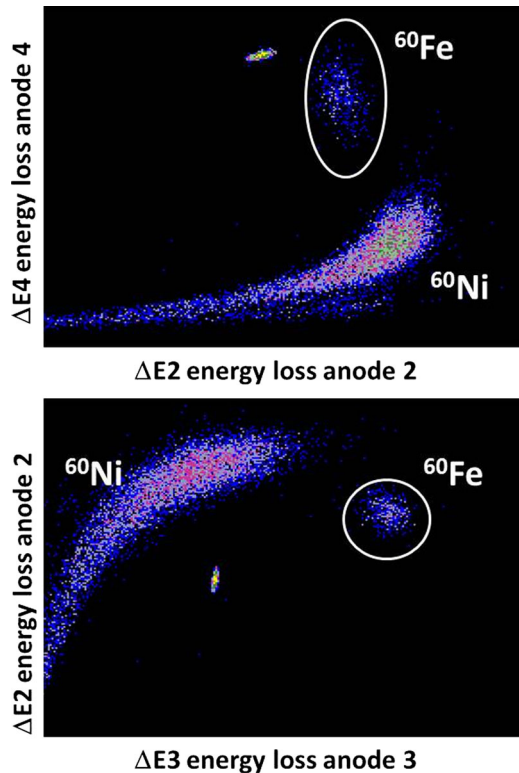
FIG. 2 (color online). Identification spectra for ^{60}Fe demonstrating a clear separation from its isobar ^{60}Ni. Displayed are third ($\Delta E3$) vs second energy-loss signal ($\Delta E2$) (lower) and second vs fourth energy-loss signals (upper plot). Note, this sample has an isotope ratio $^{60}\text{Fe}/^{\text{nat}}\text{Fe}$ of ~10^{-12}, background levels are at $< 10^{-16}$, and the samples used for the half-life measurements were $> 10^{-9}$ (the small third peak originates from a pulser signal).

TABLE III. Measured values for the determination of the number of ^{60}Fe-atoms (the ^{55}Fe-data are valid for 1/1/2010).

$R_{60/56}$(Fe-4)	$(1844 \pm 50) \times 10^{-12}$ at/at
$R_{55/56}$(Fe-4)	$(449 \pm 9) \times 10^{-12}$ at/at
^{60}Fe/^{55}Fe	(4.11 ± 0.14) at/at
$R_{55/56}$(Fe-4)/$R_{55/56}$(A0)	(0.95 ± 0.02) at/at
$R_{55/56}$(A0)	$(537 \pm 8) \times 10^{-12}$ at/at
A_{55}(Fe-1)	$(2.219 \pm 0.076) \times 10^6$ Bq
N_{60}(Fe-1)	$(1.15 \pm 0.05) \times 10^{15}$ at

N_{55}(Fe-4)/N_{55}(A0) $= 0.96 \pm 0.03$. Similarly, from LSC, using Fe-1 (Fe-2) and the dilution factor of 1000 (100) to Fe-4, we deduce 0.94 ± 0.03 (see the Supplemental Material [41], Table T1) confirming AMS at ANU and in general the method applied at different facilities.

We obtain for Fe-4 a mean absolute isotope ratio $R_{60/56} = (1.844 \pm 0.050) \times 10^{-9}$ and $R_{55/56} = (4.49 \pm 0.09) \times 10^{-10}$ from AMS at ANU, resulting in ^{60}Fe/^{55}Fe $= 4.11 \pm 0.14$ (Table III). This gives N_{60}(Fe-4) $= (1.15 \pm 0.05) \times 10^{12}$ and from the dilution series then N_{60}(Fe-1) $= (1.15 \pm 0.05) \times 10^{15}$ ^{60}Fe atoms for Fe-1 [Eq. (3)]. Applying Eq. (4), we obtain N_{60}(Fe-1) $= (1.14 \pm 0.05) \times 10^{15}$ ^{60}Fe atoms, resulting in an average value of $(1.145 \pm 0.050) \times 10^{15}$ ^{60}Fe atoms. Since the sample for the ^{60}Fe activity measurement is larger by the factor 0.65005 g/0.30120 g $= 2.1582$, the average number becomes $N_{60Fe} = (2.47 \pm 0.11) \times 10^{15}$ ^{60}Fe atoms (the individual uncertainty contributions are listed in the Supplemental Material [41], Table T3.).

Combining A_{60Fe} with N_{60Fe}, we obtain from Eq. (2) the half-life value of ^{60}Fe: $t_{1/2}(^{60}\text{Fe}) = \ln 2 \times N_{60Fe}/A_{60Fe} = \ln 2 \times 2.47 \times 10^{15}/21.72 \text{ s} = 7.891 \times 10^{13} \text{ s} = (2.50 \pm 0.12) \times 10^6$ yr.

Our result essentially confirms the measurement of Rugel et al. [28], but contradicts the earlier value of Ref. [27]. Assuming that the γ-activity measurement was correct in both experiments, unknown losses in AMS led to a lower number of ^{60}Fe atoms, and consequently to a shorter half-life. On the basis of the current result, we can calculate a weighted mean of the precise measurement of Ref. [28] and the present value as the half-life of ^{60}Fe: $t_{1/2}(^{60}\text{Fe}) = (2.60 \pm 0.05) \times 10^6$ yr.

To summarize, the most recent two measurements, using rather different techniques, agree well with each other. Hence, a more reliable value is now available for astrophysical applications. In particular, the number of ^{60}Fe atoms present in the ISM is calculated from observations of its decay rate (through ^{60}Co) which is inversely proportional to the half-life value [2]. Thus the large change of 76% between Refs. [27] and [28] led to considerable uncertainty in this quantity. It impacts evaluations of ^{60}Fe injections in the ESS [45,46]. Further, the amount of ^{60}Fe in a deep-sea crust sample, measured for a time ~ 2–3×10^6 yr in the past [15,16], requires a decay correction for

about one half-life. Thus, a similar uncertainty in the ^{60}Fe fluence was inherent to this finding. It also affected the uncertainty of a half-life-dependent ^{60}Fe-standard material for use in AMS. Our new mean half-life value reduces this deficiency to a few percent. With respect to the difficulty of performing measurements of long half-lives, it will be important to see whether the additional efforts presented in Refs. [31,32] will support the current consensus value.

[1] E. Uberseder et al., Measurement of the ^{60}Fe$(n, \gamma)^{61}$Fe Cross Section at Stellar Temperature, Phys. Rev. Lett. **102**, 151101 (2009).

[2] W. Wang, M. J. Harris, R. Diehl, H. Halloin, B. Cordier, A. W. Strong, K. Kretschmer, J. Knödlseder, P. Jean, G. G. Lichti, J. P. Roques, S. Schanne, A. von Kienlin, G. Weidenspointner, and C. Wunderer, SPI observations of the diffuse ^{60}Fe emission in the galaxy, Astron. Astrophys. **469**, 1005 (2007).

[3] R. Diehl, Nuclear astrophysics lessons from INTEGRAL, Rep. Prog. Phys. **76**, 026301 (2013).

[4] A. Shukolyukov and G. W. Lugmair, Live iron-60 in the early solar system, Science **259**, 1138 (1993).

[5] A. Shukolyukov and G. W. Lugmair, ^{60}Fe in eucrites, Earth Planet. Sci. Lett. **119**, 159 (1993).

[6] G. Quitté, A. N. Halliday, B. S. Meyer, A. Markowski, Ch. Latkoczy, and D. Günther, Correlated iron 60, nickel 62, and zirconium 96 in refractory inclusion and the origin of the solar system, Astrophys. J. **655**, 678 (2007).

[7] Y. Guan, G. R. Huss, and L. A. Leshin, ^{60}Fe-^{60}Ni and ^{53}Mn-^{53}Cr isotopic systems in sulfides from unequilibrated enstatite chondrites, Geochim. Cosmochim. Acta **71**, 4082 (2007)

[8] F. Moynier, J. Blichert-Toft, P. Telouk, J.-M. Luck, and F. Albarède, Comparative stable isotope geochemistry of Ni, Cu, Zn, and Fe in chondrites and iron meteorites, Geochim. Cosmochim. Acta **71**, 4365 (2007).

[9] M. Bizzarro, D. Ulfbeck, A. Trinquier, K. Thrane, J. N. Connoly, and B. S. Meyer, Evidence for a late supernova injection of ^{60}Fe into the protoplanetary disk, Science **316**, 1178 (2007).

[10] G. Quitte, A. Markowski, Ch. Latkoczy, A. Gabriel, and A. Pack, Iron-60 heterogeneity and incomplete isotope mixing in the early solar system, Astrophys. J. **720**, 1215 (2010).

[11] H. Tang and N. Dauphas, Abundance distribution, and origin of ^{60}Fe in the solar protoplanetary disk, Earth Planet. Sci. Lett. **359**, 248 (2012).

[12] H. Tang and N. Dauphas, ^{60}Fe-^{60}Ni chronology of core formation in Mars, Earth Planet. Sci. Lett. **390**, 264 (2014).

[13] G. J. Wasserburg, M. Busso, R. Gallino, and K. M. Nollett, Short-lived nuclei in the early solar system: Possible AGB sources, Nucl. Phys. **A777**, 5 (2006).

[14] S. Mostefaoui, G. W. Lugmair, P. Hoppe, and A. El Goresy, Evidence for ^{60}Fe in meteorites, New Astron. Rev. **48**, 155 (2004).

[15] K. Knie, G. Korschinek, T. Faestermann, E. A. Dorfi, G. Rugel, and A. Wallner, ^{60}Fe Anomaly in a Deep-Sea Manganese Crust and Implications for a Nearby Supernova Source, Phys. Rev. Lett. **93**, 171103 (2004).

[16] C. Fitoussi et al., Search for Supernova-Produced ^{60}Fe in a Marine Sediment, Phys. Rev. Lett. **101**, 121101 (2008).

[17] J. Feige, A. Wallner, S. R. Winkler, S. Merchel, L. K. Fifield, G. Korschinek, and D. Breitschwerdt, The search for supernova-produced radionuclides in terrestrial deep-sea archives, Pub. Astron. Soc. Aust. **29**, 109 (2012).

[18] J. Feige, A. Wallner, L. K. Fifield, R. Golser, G. Korschinek, S. Merchel, G. Rugel, P. Steier, and S. R. Winkler, AMS measurements of cosmogenic and supernova-ejected radionuclides in deep-sea sediment cores, Eur. Phys. J. Web Conf. **63**, 03003 (2013).

[19] S. Bishop and R. Egli, Discovery prospects for a supernova signature of biogenic origin, Icarus **212**, 960 (2011).

[20] M. Lugaro, C. L. Doherty, A. I. Karakas, S. T. Maddison, K. Liffman, D. A. Garcia-Hernandez, L. Siess, and J. C. Lattanzio, Short-lived radioactivity in the early solar system: The super-AGB star hypothesis, Meteorit. Planet. Sci. **47**, 1998 (2012).

[21] R. Diehl, N. Prantzos, and P. von Ballmoos, Astrophysical constraints from gamma-ray spectroscopy, Nucl. Phys. **A777**, 70 (2006).

[22] G. J. Wasserburg and D. A. Pappanastassiou, Some Short-Lived Nuclides in the Early Solar System: A Connection with Placental ISM, Essays in Nuclear Astrophysics, edited by, C. A. Barnes, D. D. Clayton, and D. N. Schramm (Cambridge University Press, New York, 1982), p. 77.

[23] J.-C. Roy and T. P. Kohman, Iron 60, Can. J. Phys. **35**, 649 (1957).

[24] T. P. Kohman and M. S. Robison, Iron-60 as a possible heat source and chronometer in the early solar system, Proceedings of the Eleventh Lunar and Planetary Science Conference, Houston, Texas, 1980 (Pergamon Press, New York, 1980), p. 564.

[25] J. K. Tuli, Nuclear data sheets for $A = 60$, Nucl. Data Sheets **100**, 347 (2003).

[26] E. Browne and J. K. Tuli, Nuclear data sheets for $A = 60$, Nucl. Data Sheets **114**, 1849 (2013).

[27] W. Kutschera, P. J. Billquist, D. Frekers, W. Henning, K. J. Jensen, X.-Z. Ma, R. Pardo, M. Paul, K. E. Rehm, R. K. Smither, and J. Yntema, Half-life of ^{60}Fe, Nucl. Instrum. Methods Phys. Res., Sect. B **5**, 430 (1984).

[28] G. Rugel, T. Faestermann, K. Knie, G. Korschinek, M. Poutivsev, D. Schumann, N. Kivel, I. Günther-Leopold, R. Weinreich, and M. Wohlmuther, New Measurement of the ^{60}Fe Half-Life, Phys. Rev. Lett. **103**, 072502 (2009).

[29] N. Kivel, D. Schumann, and I. Günther-Leopold, Quantification of ^{60}Fe atoms by MC-ICP-MS for the redetermination of the half-life, Anal. Bioanal. Chem. **405**, 2965 (2013).

[30] D. Schumann and J. Neuhausen, Accelerator waste as a source of exotic radionuclides, J. Phys. G **35**, 014046 (2008).

[31] R. Dressler et al., Laboratory of Radiochemistry and Environmental Chemistry, Paul Scherrer Institute (Switzerland) Annual Report 2011, p. 48; manuscript in preparation.

[32] K. Ostdiek et al., Measurement the half life of ^{60}Fe for stellar and early solar system models, Proceedings of the 13th International Conference on Accelerator Mass Spectrometry (to be published).

[33] H. A. Synal, Developments in accelerator mass spectrometry, Int. J. Mass Spectrom. **349–350**, 192 (2013).

[34] W. Kutschera, Applications of accelerator mass spectrometry, Int. J. Mass Spectrom. **349–350**, 203 (2013).

[35] N. Kivel, H.-D. Potthast, and D. Schumann, Separation of isobaric interferences in high resolution-inductively coupled plasma-mass spectrometry (HR-ICP-MS) (to be published).

[36] N. Kinoshita et al., A shorter ^{146}Sm half-life and its implications for the history of the early solar system, Science **335**, 1614 (2012).

[37] H. Junde, Nuclear data sheets for $A = 55$, Nucl. Data Sheets **109**, 787 (2008); H. Schoetzig, Half-life and x-ray emission probabilities of ^{55}Fe, Appl. Radiat. Isot. **53**, 469 (2000).

[38] A. Wallner et al., High-sensitivity isobar-free AMS measurements and reference materials for ^{55}Fe, ^{68}Ge and ^{202g}Pb, Nucl. Instrum. Methods Phys. Res., Sect. B **294**, 374 (2013).

[39] G. Korschinek, D. Mueller, T. Faestermann, A. Gillitzer, E. Nolte, and M. Paul, Trace analysis of ^{55}Fe in biosphere and technology by means of AMS, Nucl. Instrum. Methods Phys. Res., Sect. B **52**, 498 (1990).

[40] A. Wallner, M. Bichler, I. Dillmann, R. Golser, F. Käppeler, W. Kutschera, M. Paul, A. Priller, P. Steier, and C. Vockenhuber, AMS measurements of ^{41}Ca and ^{55}Fe at VERA: Two radionuclides of astrophysical interest, Nucl. Instrum. Methods Phys. Res., Sect. B **259**, 677 (2007).

[41] See Supplemental Material at http://link.aps.org/supplemental/10.1103/PhysRevLett.114.041101 for details on the AMS measurements.

[42] A. Wallner et al., Search for a live supernova signature of ^{60}Fe in deep-sea sediments and a new half-life measurement of ^{60}Fe (to be published).

[43] L. K. Fifield, S. Tims, T. Fujioka, W. Hoo, and S. Everett, Accelerator mass spectrometry with the 14UD accelerator at the Australian National University, Nucl. Instrum. Methods Phys. Res., Sect. B **268**, 858 (2010).

[44] M. Paul, B. G. Glagola, W. Henning, J. G. Keller, W. Kutschera, Z. Liu, K. E. Rehm, B. Schneck, and R. H. Siemssen, Heavy ion separation with a gas-filled magnetic spectrograph, Nucl. Instrum. Methods Phys. Res., Sect. A **277**, 418 (1989).

[45] A. P. Boss, Evolution of the solar nebula: VIII, Spatial and temporal heterogeneity of short-lived radioisotopes and stable oxygen isotopes, Astrophys. J. **660**, 1707 (2007).

[46] N. Dauphas, D. L. Cook, A. Sacarabany, C. Fröhlich, A. M. Davis, M. Wadhwa, A. Pourmand, T. Rauscher, and R. Gallino, Iron 60 evidence for early injection and efficient mixing of stellar debris in the protosolar nebula, Astrophys. J. **686**, 560 (2008).